MODELING THE IMPACT OF ELECTRIC VEHICLE CHARGING STATIONS (EVCSs) ON THE ELECTRICAL GRID AND OPTIMIZING THEIR PLACEMENT

MUSTAFA NURMUHAMMED · OZAN AKDAĞ · TEOMAN KARADAĞ

BIDGE Publications

Modeling the Impact of Electric Vehicle Charging Stations (EVCSs) on the Electrical Grid and Optimizing Their Placement

Author: Mustafa Nurmuhammed, Ozan Akdağ, Teoman Karadağ

ISBN: 978-625-8995-04-6

1st Edition

Page Layout By: Gozde YUCEL

Publication Date: 22.03.2026

BIDGE Publications

Certificate No: 71374

www.bidgeyayinlari.com.tr - bidgeyayinlari@gmail.com
Krc Bilişim Ticaret ve Organizasyon Ltd. Şti.
Güzeltepe Mahallesi Abidin Daver Sokak Sefer Apartmanı No: 7/9 Çankaya / Ankara

İçindekiler

Introduction

EVs first emerged in the late nineteenth century and initially saw limited adoption. However, interest in EVs declined with the advancement of internal combustion engine technologies, the decreasing cost of petroleum, and the expansion of mass production capabilities (1). The growing demand for long-distance transportation further accelerated this decline. Although the oil crisis of the 1970s briefly revived interest, the real transformation began after 2008. In particular, advances in battery technologies led to a rapid increase in EV sales, with significant growth rates.

The widespread adoption of EVs is influenced by many factors such as charging infrastructure, driving range, charging time, and cost of ownership. In addition, government incentives and environmental concerns play a significant role. In this context, charging stations have become a critical component of the EV market. While home charging can take between 18 and 36 hours, fast-charging stations can reduce this time to approximately 30 minutes or less.

Today, the increasing deployment of high-power fast-charging stations, typically in the range of 350–400 kW, enables multiple vehicles to be charged simultaneously. However, this also imposes a substantial additional load on the power distribution network. For instance, charging four vehicles simultaneously at 250 kW results in a load of approximately 1 MW, which is equivalent to the monthly electricity consumption of around 120 households (2). Such sudden load increases may lead to transformer overloading and instability in the power system (3). Moreover, charging during peak hours can cause load increases of up to 68% on transformers (4). Energy consumption varies both throughout the day and seasonally (5), with these variations being more pronounced in tourism regions (6). As EV adoption continues to rise, these fluctuations are expected to become even more critical (7–10).

The growing penetration of EVs may lead to sudden increases in energy demand, voltage drops, and phase imbalances in the grid (11–14). Therefore, the unplanned deployment of charging infrastructure poses significant risks to the stability and reliability of the power distribution system.

In the literature, studies on electric vehicle (EV) charging stations are generally examined under two main categories: the optimal siting of charging stations and their impacts on the power distribution network (15). Due to the high installation and operational costs of charging stations, cost has been widely considered as a primary optimization parameter in many studies. In this context, optimal placement is achieved by jointly evaluating factors such as power losses, investment costs, and user accessibility costs (16).

Harmonics generated during EV charging can negatively affect power quality and lead to degradation in system performance (17–23). This issue may impose additional stress on distribution lines and transformers, thereby reducing service quality (17).

Smart grid structures enable more efficient energy management. Within this framework, Vehicle-to-Grid (V2G) technology allows EVs to function not only as energy consumers but also as energy providers (24–29). In such systems, EV batteries can support the grid, particularly during peak demand periods. The literature shows that this approach improves voltage profiles and provides economic benefits (25).

Load forecasting is a critical research area for analyzing the impact of EVs on the distribution network (30–33). Some studies develop future-oriented scenarios (30), while others perform analyses based on fixed load assumptions (16) (34).

The integration of renewable energy sources into charging infrastructure is an important approach to reducing the burden on the power system (35). Charging EVs using sources such as solar energy is a common example (36)(37). However, the intermittent nature of renewable energy generation complicates grid management. Therefore, such systems must be considered together with energy storage solutions and intelligent management strategies.

With appropriate system design and management strategies in power distribution networks, the balance between generation and consumption can be optimized. EVs can be charged via a microgrid powered by renewable energy sources. In this structure, energy storage systems, residential energy infrastructure, and backup generators are managed in an integrated manner through a microgrid controller. The integration of high-capacity renewable energy sources into distribution networks requires large-scale energy storage systems. At this point, EV batteries can function as distributed energy storage units. In particular, studies have shown that EV batteries play an effective role in mitigating fluctuations in wind energy generation (38)(39)(40). Furthermore, the impact of charging stations on energy consumption in commercial areas has been analyzed, and it has been demonstrated that solar energy integration can help reduce these effects (41)(42). However, in scenarios involving renewable energy, load uncertainty remains a significant factor, and both demand and generation patterns must be jointly considered during the planning phase (43).

The high power demand during EV charging increases active power losses in the distribution network. Therefore, the proper placement and capacity selection of charging stations play a critical role in minimizing these losses. The literature provides detailed analyses of the impacts of charging stations on power flow, short-circuit levels, and protection systems (44).

Many studies formulate optimization problems by jointly considering parameters such as power loss, voltage deviation, and cost (45–47). Additionally, charging/discharging strategies and energy management approaches have been shown to effectively reduce power losses and improve system reliability (48–51).

In studies employing various optimization methods, minimizing power loss has been one of the primary objectives. For example, the placement of renewable energy-supported charging stations has been optimized using metaheuristic algorithms (52). Studies utilizing probabilistic load modeling aim to minimize losses from both the distribution system and EV perspectives (53). Moreover, recent studies have improved solution performance by employing next-generation optimization algorithms (54–57). Some studies have applied hybrid optimization techniques to simultaneously minimize power loss and voltage deviation (58)(59). Overall, the literature indicates that the uncontrolled placement of EV charging stations can have adverse effects on the distribution network, while optimization-based approaches can significantly mitigate these impacts (12,60–67).

Problem Formulation and System Modeling

The optimal placement of electric vehicle charging stations (EVCSs) in distribution networks can be formulated as a constrained optimization problem. The objective is to determine suitable buses and charging capacities while maintaining acceptable grid performance. In practice, an effective placement must balance user accessibility with technical requirements such as power quality, energy efficiency, and voltage stability.

This problem is particularly challenging because distribution networks are typically radial, operate at lower voltage levels, and are sensitive to sudden load changes. Integrating high-power charging stations into weak parts of the network may lead to voltage violations, increased losses, or overloading. Therefore, the formulation must explicitly incorporate grid performance indices and operational constraints.

In this section, EVCS placement is modeled as a multi-objective optimization problem, where the goal is to identify locations that provide the best overall system performance under given constraints.

The distribution system is represented as a radial network composed of buses and branches. Each bus may correspond to a load point or a connection node. Load flow analysis is used to calculate bus voltages, branch currents, and power losses.

Due to their structure, radial systems are prone to voltage drops along feeders, especially under heavy loading. The integration of EVCSs increases demand, which raises current levels and further exacerbates voltage drops. Therefore, accurate modeling of voltages and power flows is essential.

The base case represents the network without EVCSs, while the modified case includes charging loads at selected buses. The optimization algorithm determines these locations and evaluates system performance accordingly.

The EVCS placement problem can be summarized as determining the optimal locations that minimize power loss and voltage deviation while maximizing voltage stability, subject to operational constraints.

This formulation provides a practical and comprehensive framework for evaluating optimization algorithms in real distribution systems.

Modeling of Electric Vehicle Charging Stations

EV charging stations are modeled as additional loads connected to selected buses. Depending on the charging type, they may represent alternating current (AC) or direct current (DC) chargers, with DC fast chargers imposing significantly higher demand.

AC charging is the default form of electricity in the power distribution network. Battery packs used in electric vehicles operate on the DC principle by nature. Therefore, to charge the battery pack in the vehicle, power in the form of AC must be converted to DC. This process is carried out by the vehicle's built-in charger which is called on-board charger (OBC). These chargers have limited power ratings due to thermal management and conversion constraints as well as limited space in the car. AC charging is commonly used at home or in public charging stations. Table 1 shows the AC charging values defined by SAE International.

Table 1 AC standards as defined by SAE International.

Charge method	Voltage (V)	Phase	Max Current (A)	Max Power (kW)
AC Level 1	120	1-phase	12	1.44
			16	1.92
AC Level 2	208 - 240	1-phase	80	19.2

DC charging is a charging method where the conversion from AC to DC takes place outside the vehicle, at the charging station or nearby area, and DC power is supplied directly to the batteries. This charging method is much faster than AC charging because a much larger amount of DC power can be obtained outside the vehicle, and it is more advantageous in terms of power loss during AC to DC conversion.

Depending on the charging power and the vehicle's charging speed, a DC charging station can charge an electric vehicle from 0% to 80% in approximately 30 minutes or less. Fast charging supports long-distance travel by reducing charging duration. To speed up charging times, many countries are investing in charging stations that can provide power of 350 kW and above. High-speed DC charging stations significantly reduce waiting time during charging. Therefore, this method stands out as one of the most efficient charging options.

Given the significant annual increase in electric vehicle sales, the number of DC charging stations is expected to increase in response to growing demand. The widespread adoption and development of charging infrastructure is considered one of the key drivers for the rapid spread of electric vehicles (68). Table 2 presents the DC output voltage, maximum current, and maximum power data defined by SAE for DC charging stations. (69).

Table 2 DC standards as defined by SAE International.

Charge Method	DC Output Voltage(V)	Max Current (A)	Max Power (kW)
DC Level 1	50 - 1000	80	80
DC Level 2	50 - 1000	400	400

The charging time of electric vehicles with any charging method is directly related to the battery capacity and the power provided by the charger. Electric vehicle manufacturers determine the charging speeds of their vehicles with AC and DC batteries to ensure trouble-free operation in different climatic conditions.

Continuous investments are being made in DC charging stations worldwide. Despite this, there is a need for DC charging stations in many parts of Europe. The cost of planned investments to meet this need is estimated to reach €20 billion over 11 years. This corresponds to approximately €1.8 billion annually. The total cost is equivalent to 3% of the European Union's road infrastructure budget. (70).

Tesla has a charging network called "Supercharger". In 2019, the third version increased the charging speed to 250 kW. This version provides 250 kW of charging power without sharing it with other vehicles. As of February 2026, more than 75,000 Superchargers were available to users worldwide. (71).

Today, there are DC charging stations that provide different power levels. Charging times vary depending on the power provided by the stations. For example, the time required to charge an electric vehicle with a 40 kWh battery capacity from 0% to 80% is given in Table 3 below (72).

Table 3 Charging type, power, and duration

Charging type	Power	Duration
Standard Charging	2.3 kW – 7.4 kW	4-14 hours
Semi-Fast Charging	22 kW	1.5 hours
Fast Charging	40-50 kW	30 minutes
Super Fast Charging	100-150 kW	15 minutes
Ultra Fast Charging	175-400 kW	5-10 minutes

The charging speed and duration of electric vehicles depend on how quickly the batteries can be charged. Significant advancements have been made in battery technology in recent years. This has led to the development and commercial use of batteries that can be charged very quickly in a short time. The average efficiency guarantee period for batteries worldwide is approximately eight to ten years. Ongoing battery research shows promise in increasing charging speeds through battery chemistries that can withstand higher currents.

In this book, EVCS loads are treated as constant power loads, representing a worst-case scenario with continuous maximum demand. Although real charging behavior is time-varying, this assumption provides a consistent basis for evaluating grid impact.

The load is defined in terms of active and reactive power. While reactive power is typically small due to near-unity power factor operation, it can be included when necessary. Additionally, candidate buses are predefined to reflect practical constraints such as land availability and regulatory limitations.

Objective Functions

The EVCS placement problem involves multiple, often conflicting, objectives. For example, placing stations near the substation can reduce losses but may not align with user demand, whereas demand-driven placement may cause voltage issues. Therefore, a multi-objective framework is required.

This study considers three widely used performance metrics:

- Minimization of active power losses
- Minimization of voltage deviation
- Maximization of voltage stability index (VSI)

These objectives collectively represent: efficiency, power quality, and system reliability.

Active Power Loss Minimization

Active power losses mainly arise from resistive effects in distribution lines. As EVCSs increase current flow, losses also increase. In radial systems, total loss depends strongly on load placement.

Minimizing these losses improves efficiency and reduces operational costs, making it a key objective in EVCS planning.

Active power loss is one of the most important criteria in determining the optimum location of electric vehicle charging stations in the distribution network. The active and total power loss in each line can be calculated as shown in Equation 1:

$$Total\ Power\ Loss = \left\{ \sum_{i=1}^{n_{branch}} I_i^2 \ R_i \right\} \tag{1}$$

where I_i is the line current, n_{branch} is the number of lines, R_i is the line resistance.

Voltage Deviation Minimization

Voltage deviation reflects how far bus voltages are from their nominal values. Distribution systems must operate within specified limits (e.g., ±5%), and violations can affect service quality. This objective aims to maintain a stable voltage profile by minimizing deviations across all buses. It is particularly important since EVCSs are often installed at buses already experiencing low voltage levels.

Significant voltage deviations or drops can occur in unplanned placements of electric vehicle charging stations. To mitigate such effects, including voltage deviation as an index value in the problem formulation will improve the voltage quality of the overall power system. Thus, reducing voltage deviations will have a positive impact on the placement problems of electric vehicle charging stations. Voltage deviation can be calculated using the formula in Equation 2. The result gives the deviation as a percentage;

$$Voltage\ Deviation = \sum_{i=1}^{n_{bus}} (1 - V_i)^{2} \times 100 \qquad (2)$$

V_i is the bus voltage, n_{bus} is the number of buses.

Voltage Stability Index Maximization

The placement of charging stations in distribution networks significantly affects voltage stability. Voltage stability refers to a system's ability to maintain its nominal operating conditions and return to its original state after a disturbance that could lead to voltage imbalance and an uncontrollable voltage drop. The VSI provides a measure of proximity to instability or collapse. VSI helps in identifying weak busbars. Maximizing VSI ensures adequate stability margins. While voltage deviation captures immediate issues, VSI reflects deeper system reliability, especially under stressed conditions. VSI can be calculated using active and reactive power equations. Equation 3 from reference (73), as given below, was used to calculate VSI values.

$$VSI_{k+1} = |V_k|^4 - 4(P_{k+1}X_k - Q_{k+1}R_k)^2 - 4(P_{k+1}R_k + Q_{k+1}X_k)^2|V_k|^2 \qquad (3)$$

In this equation, V_k and V_{k+1} represent the voltage values of the k-th and (k+1)th buses, respectively, while P_{k+1} and Q_{k+1} denote active and reactive power at bus *k+1*.

Combined Fitness Function

To enable optimization, the multiple objectives are combined into a single weighted fitness function. This approach allows the algorithm to evaluate each solution using a unified metric.

The combined function includes weighted terms for power loss, voltage deviation, and voltage stability. The weights are selected to achieve balanced performance, although they can be adjusted depending on operational priorities.

The multi-objective function to be used in the electric vehicle charging station placement problem using the index values mentioned above is given in Equation 4:

$$min\left\{ w_1 \times f_1 + w_2 \times f_2 + \frac{w_3}{f_3} \right\} \tag{4}$$

Here, w_1, w_2 and w_3 are weighting factors and represent the coefficients of the functions f_1, f_2 and f_3. The objective function f_1, shown in Equation 5 below, is used to minimize the power loss value.

$$f_1 = min\left\{ \sum_{i=1}^{n_{branch}} I_i^2 \, R_i \right\} \tag{5}$$

The objective function f_2, shown in Equation 6, is used to minimize the voltage deviation.

$$f_2 = min\left\{ \sum_{i=1}^{n_{max}} (1 - V_i)^{\,2} \times 100 \times MVAb \right\} \tag{6}$$

Ideally, the VSI value should be greater than 0. However, the higher this value, the better the stability of the system. To calculate the VSI value, the objective function in Equation 7 is used.

$$VSI = max\{2V_k^2 V_{k+1}^2 - 2V_{k+1}^2 (P_{k+1} r + Q_{k+1} x) - |Z|^2 (P_{k+1}^2 + Q_{k+1}^2)\} \tag{7}$$

Among all the VSI values, the lowest VSI value represents the weakest link in terms of system stability. The lowest VSI value for this bus is found using Equation 8. Then, the constant w_3 in Equation 4 is divided by this value.

$$f_3 = min\{VSI\} \tag{8}$$

Constraints of the Optimization Problem

The optimization is subject to several constraints that ensure feasible and safe operation: these constraints prevent unrealistic or unsafe solutions.

The following constraints (Equations 9-12) are used to ensure optimum power flow, including minimum voltage, power, and voltage stability of the distribution network.

$$0 < VS\dot{I}_i \quad i = 1,2, \ldots \ldots . Ng \tag{9}$$

$$Active\ Power\ P_i^{min} \leq P_i \leq P_i^{max} \quad i = 1,2, \ldots Ng \tag{10}$$

$$Reactive\ Power\ Q_i^{min} \leq Q_i \leq Q_i^{max} \quad i = 1,2, \ldots Ng \tag{11}$$

$$Bus\ Voltage\ V_i^{min} \leq |V_i| \leq V_i^{max} \quad i = 1,2, \ldots Nb \tag{12}$$

N: number of buses; P_i: active power of bus i; Q_i: reactive power of bus i; V_i: voltage of bus i.

EVCS Placement Case Studies

EVCS placement in distribution networks involves nonlinear load flow constraints, voltage limits, and practical feasibility considerations.

Algorithms are tested on three systems:

- IEEE-33 bus radial distribution network
- IEEE-69 bus radial distribution network
- A real 10-bus distribution system (Hatay case)

These case studies assess both technical performance and real-world applicability.

IEEE-33 Bus Distribution System

The distribution system is divided into zones, as in studies (34,47,74,75). The schematic and zones of the IEEE-33 bus test distribution network are shown in Figure 1.

Figure 1 IEEE-33 bus test system

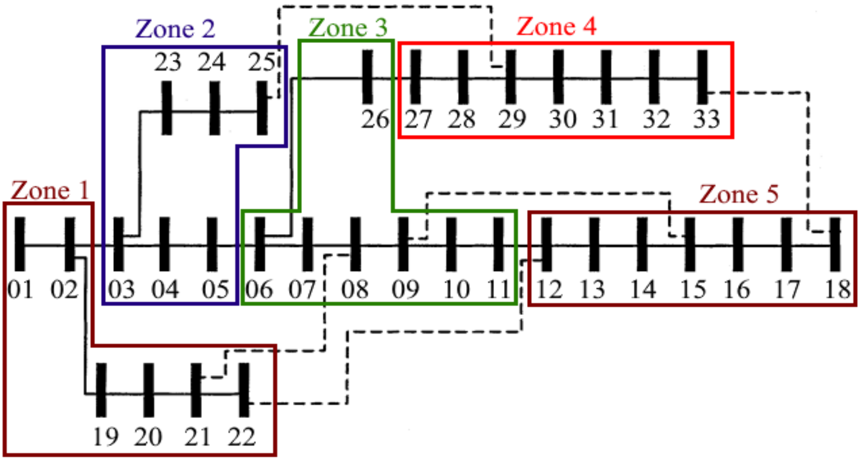

In this section, the multi-objective function in Equation 4 is used for the optimum integration (positioning) of electric vehicle charging stations into the distribution network using optimization algorithms. The multi-objective function includes active power losses, voltage deviation, and VSI parameters. These indices were combined into a weighted objective function. Since the AC and DC charging power is different for each electric vehicle, electric vehicle charging stations with various power levels ranging from 50 kW to 150 kW were used. For zones 1 to 5, the active power values of the stations were accepted as 120 kW, 75 kW, 150 kW, 100 kW, 50 kW, and the reactive power values as 75 kVAR, 47 kVAR, 95 kVAR, 63 kVAR, and 32 kVAR. In each zone, a single bus is selected for charging station placement.

For comparison purposes, the weighting coefficients of the objective function were set as w_1=0.4504, w_2=905.9343, and w_3=95.0525. The weighting coefficients were selected so that the ideal value of each index corresponds to 100, yielding a best possible total fitness of 300.

The formulated objective function was compared with well-known, classical and novel optimization algorithms with proven effectiveness. These algorithms include the Honey Badger Algorithm (HBA), Sine Cosine Algorithm (SCA), Social Network Search (SNS), Genetic Algorithm (GA), Particle Swarm Optimization (PSO), Butterfly Optimization Algorithm (BOA), Hybrid Particle Swarm Optimization Butterfly Optimization (HPSOBOA), and Tunicate Swarm Algorithm (TSA) (76–83). In addition to the above algorithms the Archimedes Optimization Algorithm (AOA)(84) and modified AOA algorithms are used. These algorithms are: Modified Archimedes Optimization Algorithm (MAOA) and Dimension-Enhanced Modified Archimedes Optimization Algorithm (MDAOA). Details of the two modified algorithms are explained at the end of this book. Comparative results are presented graphically in Figure 2 and tabularly in Table 4. Results were calculated using a population size N=30, a maximum number of iterations t_{max}=100, and 30 studies. Standard AOA has different C_3 and C_4 values for engineering problems and standard optimization functions. Since the recommended values for engineering problems provide better results for AOA, these recommended values were used when comparing with the modified AOA.

Table 4 Comparative results of optimization algorithms for the deployment of electric vehicle charging stations on the IEEE-33 bus test distribution network.

	Mean	Std. Deviation	Median	Maximum
AOA	3.12E+02	6.13E+00	3.12E+02	3.26E+02
MAOA	3.01E+02	2.75E+00	3.00E+02	3.15E+02
MDAOA	3.01E+02	2.22E+00	3.00E+02	3.12E+02
HBA	3.02E+02	4.48E+00	3.00E+02	3.14E+02
SCA	3.01E+02	1.46E+00	3.00E+02	3.08E+02
SNS	3.02E+02	4.20E+00	3.00E+02	3.12E+02
GA	3.07E+02	6.14E+00	3.12E+02	3.14E+02
PSO	3.19E+02	5.76E+00	3.20E+02	3.35E+02
BOA	3.27E+02	6.77E+00	3.30E+02	3.39E+02
HPSOBOA	3.35E+02	6.16E+00	3.34E+02	3.47E+02
TSA	3.13E+02	1.24E+01	3.09E+02	3.42E+02

The best locations yielding the minimum fitness value are buses 1, 3, 12, 26, and 27. In 30 runs of the objective function with AOA, the minimum fitness value was calculated as 3.03E+02, the average as 3.12E+02, and the maximum as 3.26E+02. Furthermore, the standard deviation for AOA was found to be 6.13E+00. Under the same conditions with MAOA and MDAOA, the minimum fitness value for the objective function was calculated as 3.00E+02 for both algorithms, and the average as 3.01E+02. Additionally, the standard deviation values for MAOA and MDAOA were calculated as 2.75E+00 and 2.22E+00, respectively. The minimum VSI value was calculated as 0.9386, and the minimum stress value as 0.9923. The convergence graphs of all algorithms for the problem are given in Figure 2.

Figure 2 Graph showing the fitness values of MAOA, MDAOA, and other optimization algorithms for the IEEE-33 bus distribution network.

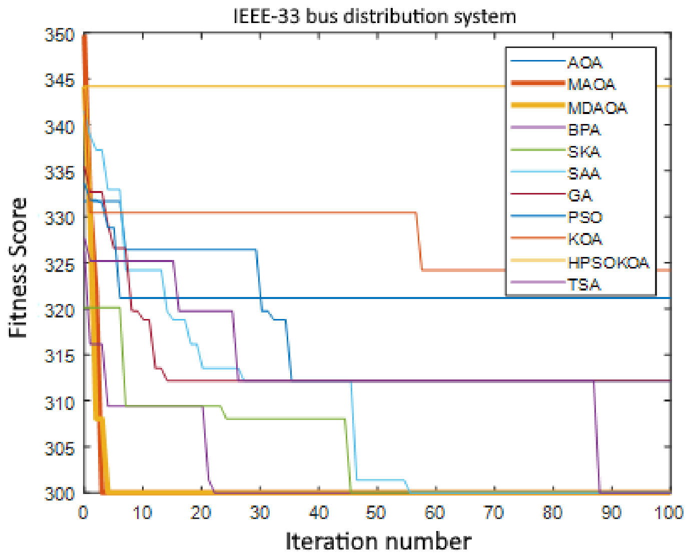

The numerical results in Table 4 and the convergence curves in Figure 2 show that the modified AOA (MAOA and MDAOA) achieved successful results when compared with other techniques. This demonstrates that MAOA can be used in the charging station placement problem, which is a significant and challenging problem in power system engineering.

The voltage details after the placement of electric vehicle charging stations are shown in Table 5.

Table 5 Bus voltages in the IEEE-33 bus test distribution network after the placement of electric vehicle charging stations.

Bus	Voltage p.u.	Bus	Voltage p.u.	Bus	Voltage p.u.
1	1.0000	12	0.9923	23	0.9982
2	0.9997	13	0.9923	24	0.9982
3	0.9982	14	0.9923	25	0.9982
4	0.9972	15	0.9923	26	0.9935
5	0.9963	16	0.9923	27	0.9931
6	0.9939	17	0.9923	28	0.9931
7	0.9937	18	0.9923	29	0.9931
8	0.9934	19	0.9997	30	0.9931
9	0.9930	20	0.9997	31	0.9931
10	0.9925	21	0.9997	32	0.9931
11	0.9924	22	0.9997	33	0.9931

According to Table 5, all bus voltages remained within operational limits.

IEEE-69 Bus Distribution System

The eight-section configuration of the IEEE 69-bus test distribution network is presented in Figure 3.

Figure 3 IEEE-69 bus test system

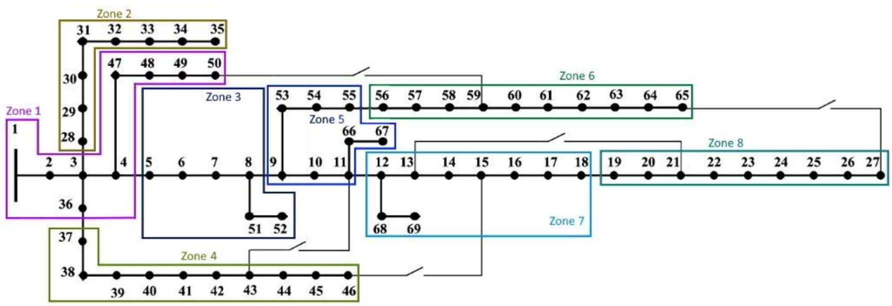

For eight zones, the active power values of the electric vehicle charging stations are 120 kW, 75 kW, 150 kW, 100 kW, 50 kW, 130 kW, 50 kW, 100 kW, and the reactive power values are 75 kVAR, 47 kVAR, 95 kVAR, 63 kVAR, 32 kVAR, 82 kVAR, 32 kVAR, and 63 kVAR. For the IEEE 69 bus test distribution network, the same power values range as in the IEEE 33 bus test system simulation were used.

The weighting coefficients of the objective function were set as w_1=0.6136, w_2=1075.0363, w_3=95.5665 (so that the best placement result for all three indices is 300).

Figure 4 shows the comparative results of AOA, MAOA, HBA, SCA, SNS, GA, PSO, BOA, HPSOBOA, and TSA for the deployment of electric vehicle charging stations to the IEEE 69-bus distribution system, while the numerical results are presented in Table 6. The results were calculated with a population size of N=30, a maximum number of iterations of 100, and 30 runs.

Table 6 Comparison of results of optimization algorithms for the deployment of electric vehicle charging stations to the IEEE-69 bus distribution system.

	Mean	Std. Deviation	Median	Maximum
AOA	3.12E+02	1.28E+01	3.09E+02	3.48E+02
MAOA	3.01E+02	1.64E+00	3.01E+02	3.08E+02
MDAOA	3.01E+02	8.44E-01	3.01E+02	3.04E+02
HBA	3.09E+02	1.54E+01	3.04E+02	3.53E+02
SCA	3.12E+02	6.25E+00	3.12E+02	3.34E+02
SNS	3.02E+02	7.21E+00	3.01E+02	3.40E+02
GA	3.02E+02	1.54E+00	3.01E+02	3.04E+02
PSO	3.21E+02	1.76E+01	3.10E+02	3.45E+02
BOA	3.37E+02	1.88E+01	3.34E+02	3.65E+02
HPSOBOA	3.63E+02	2.21E+01	3.67E+02	4.02E+02
TSA	3.36E+02	2.69E+01	3.38E+02	4.02E+02

The best locations yielding the minimum fitness value are bus numbers 1, 5, 9, 12, 19, 28, 37, and 56.

For 30 runs of the objective function with AOA, the mean was calculated as 3.12E+02, the median as 3.09E+02, and the maximum as 3.48E+02. The standard deviation for AOA was also found to be 1.28E+01. For MAOA, in 30 runs under the same conditions, the mean was calculated as 3.01E+02, the median as 3.01E+02, and the maximum as 3.08E+02 for the objective function. The standard deviation for MAOA was also found to be 1.64E+00. For MDAOA, the mean was calculated as 3.01E+02, the median as 3.01E+02, and the maximum as 3.04E+02 for the objective function. The standard deviation for MDAOA was also found to be 8.44E-01.

The voltage details after the installation of electric vehicle charging stations are given in Table 7.

Table 7 Bus voltages in the IEEE-69 bus system after the installation of electric vehicle charging stations.

Bus	Voltage p.u.	Bus	Voltage p.u.	Bus	Voltage p.u.
1	1.0000	24	0.9935	47	1.0000
2	1.0000	25	0.9935	48	1.0000
3	1.0000	26	0.9935	49	1.0000
4	1.0000	27	0.9935	50	1.0000
5	0.9999	28	1.0000	51	0.9979
6	0.9990	29	1.0000	52	0.9979
7	0.9982	30	1.0000	53	0.9977
8	0.9979	31	1.0000	54	0.9976
9	0.9978	32	1.0000	55	0.9974
10	0.9976	33	1.0000	56	0.9972
11	0.9974	34	1.0000	57	0.9963
12	0.9966	35	1.0000	58	0.9963
13	0.9958	36	1.0000	59	0.9963
14	0.9950	37	0.9998	60	0.9963
15	0.9942	38	0.9997	61	0.9963
16	0.9940	39	0.9997	62	0.9963
17	0.9937	40	0.9997	63	0.9963
18	0.9937	41	0.9997	64	0.9963
19	0.9935	42	0.9997	65	0.9963
20	0.9935	43	0.9997	66	0.9974
21	0.9935	44	0.9997	67	0.9974
22	0.9935	45	0.9997	68	0.9966
23	0.9935	46	0.9997	69	0.9966

The minimum VSI value was calculated as 0.9353, and the minimum voltage value as 0.9935. The results show that MAOA and MDAOA achieve successful results with minimum standard deviation. The convergence curves of the minimum results of 11 algorithms, including AOA, MAOA, and MDAOA, are given in Figure 4.

Figure 4 Comparison of the results of optimization algorithms for the placement of electric vehicle charging stations on the IEEE-69 bus test distribution network.

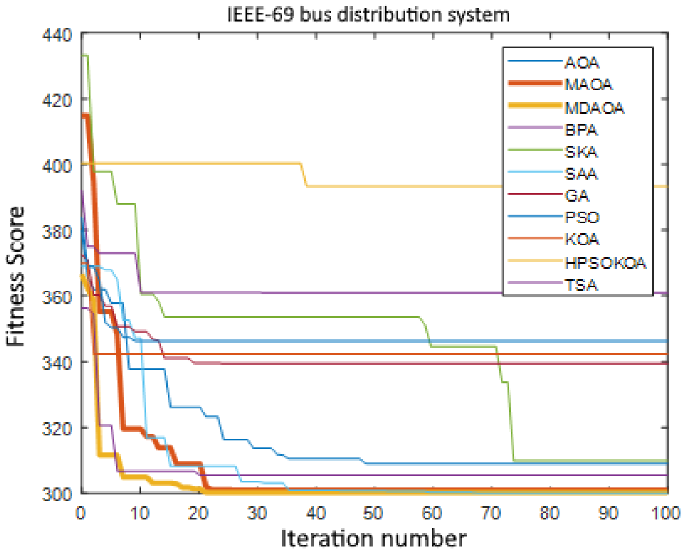

Figure 4 and Table 6 clearly show that MAOA and MDAOA achieve better results compared to other techniques.

Real Distribution Network (Hatay 10-Bus System)

The charging station placement problem with AOA and modified AOA (MAOA and MDAOA) was applied to the 10-bus Hatay distribution network. This network is divided into two regions. The first region contains buses 2, 3, 4, 5, 8, and 9. The second region contains buses 1, 6, 7, and 10. The divided version of the Hatay 10-bus distribution network is presented in Figure 5.

Figure 5 The 10-bus Hatay distribution network.

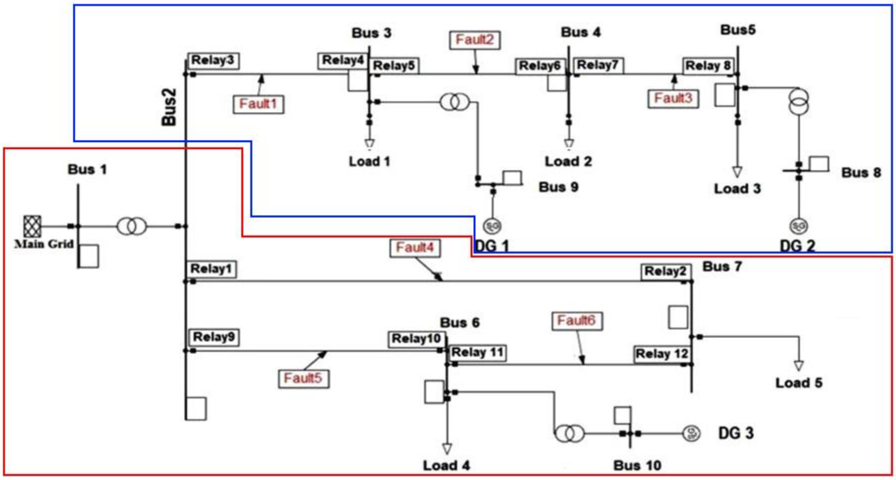

For the two regions, the active power values of electric vehicle charging stations were assumed to be 120 kW, 75 kW, and the reactive power values were assumed to be 75 kVAR, 47 kVAR. The comparison of the numerical results obtained from AOA, MAOA, MDAOA, and eight other optimization algorithms for the placement of electric vehicle charging stations in the 10-bus Hatay distribution network is shown in Table 8.

Table 8 Comparison of the results of optimization algorithms for the placement of electric vehicle charging stations in the Hatay 10-bus distribution system.

	Mean	Std. Deviation	Median	Maximum
AOA	3.19E+02	3.06E+01	3.00E+02	3.96E+02
MAOA	3.00E+02	0	3.00E+02	3.00E+02
MDAOA	3.00E+02	0	3.00E+02	3.00E+02
HBA	3.07E+02	2.36E+00	3.00E+02	3.96E+02
SCA	3.00E+02	0	3.00E+02	3.00E+02
SNS	3.00E+02	0	3.00E+02	3.00E+02
GA	3.24E+02	4.05E+00	3.20E+02	3.96E+02
PSO	3.48E+02	6.63E+00	3.00E+02	4.07E+02
BOA	3.00E+02	0	3.00E+02	3.00E+02
HPSOBOA	3.00E+02	0	3.00E+02	3.00E+02
TSA	3.06E+02	52.671	3.00E+02	3.96E+02

For AOA, the minimum fitness value for 30 runs of the objective function was calculated as 3.00E+02, the mean as 3.19E+02, the median as 3.00E+02, and the maximum as 3.96E+02. Furthermore, the standard deviation for AOA was found to be 3.06E+01. For MAOA and MDAOA, under the same conditions and after 30 runs, the minimum fitness value for the objective function was calculated as 3.00E+02, the mean as 3.00E+02, the median as 3.00E+02, and the maximum as 3.00E+02. Additionally, the standard deviation for the modified algorithms MAOA and MDAOA was calculated as 0. A comparison of the convergence curve graphs of the 11 optimization algorithms is shown in Figure 6.

Figure 6 Comparison of fitness value convergence curve graphs of optimization algorithms for the 10-bus virtual model of the Hatay distribution network.

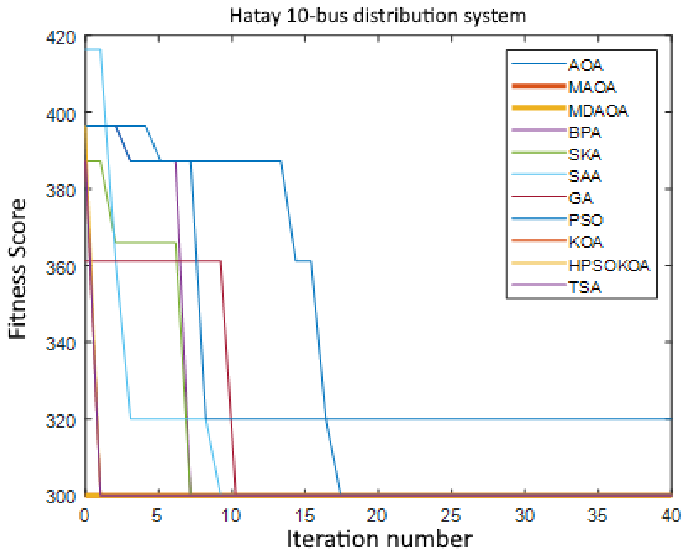

The results show that MAOA and MDAOA achieve successful results with low standard deviation values compared to other techniques. This indicates that MDAOA can be used in the electric vehicle charging station placement problem, which is critical in power system engineering from a distribution system perspective.

Comparative Discussion

Across all case studies, the following conclusions emerge:

- Uncontrolled EVCS placement leads to significant losses and voltage degradation
- MAOA improves performance by maintaining diversity and reducing early convergence
- MDAOA consistently achieves the best results due to enhanced exploration

- Optimized placement improves voltage stability and overall reliability
- Network topology and loading conditions strongly influence optimal solutions

Overall, the results confirm that the two modified AOA algorithms—particularly MDAOA—are both technically effective and practically applicable for EVCS planning in distribution networks.

Case studies on IEEE-33, IEEE-69, and the Hatay network demonstrate the practical impact of optimization. Without coordination, EVCS integration increases power losses and voltage drops. Optimized placement significantly mitigates these effects.

Power Loss Reduction: Both MAOA and MDAOA reduce losses by distributing charging demand more effectively. MDAOA achieves the highest reduction, indicating better identification of globally optimal placements. From an operational perspective, even small loss reductions can result in meaningful cost savings.

Voltage Profile Improvement: Voltage deviation is highly sensitive to EVCS placement. Optimized solutions improve voltage profiles, particularly in radial systems with long feeders.

MDAOA consistently provides the best results by avoiding weak buses and selecting locations that balance accessibility with electrical constraints. This reduces the need for costly grid reinforcements.

Voltage Stability Enhancement: Voltage stability is critical for long-term reliability. Results show that optimized placement improves stability margins, with MDAOA achieving the highest VSI values. This indicates that the algorithm not only addresses immediate voltage issues but also supports future load growth.

MDAOA Performs Better

The superior performance of MDAOA can be explained by three main factors:

- Dimension enhancement, which expands the search space and helps escape local optima
- Improved acceleration updates, which reduce dominance of a single solution
- Better diversity preservation, allowing sustained exploration

These features enable MDAOA to consistently identify higher-quality solutions across different problem types.

Practical Implications

From a practical perspective, several conclusions can be drawn:

- EVCS placement should not rely solely on demand; grid constraints must be considered
- Optimization-based planning can reduce losses and improve voltage stability without major infrastructure upgrades
- Reliable algorithms are essential, as inconsistent results are not suitable for real planning
- Including stability indices provides a more forward-looking and resilient planning strategy

MDAOA's consistent performance makes it a strong candidate for decision-support applications in distribution systems.

Limitations

Despite the strong results, some limitations exist. EVCS demand is modeled as constant, whereas real demand is time-varying and stochastic. Future studies could incorporate probabilistic or time-series models.

Additionally, the current framework focuses primarily on grid performance. A more comprehensive approach could integrate transportation demand, GIS-based analysis, and economic factors.

Summary of Results

In summary:

- Uncontrolled EVCS placement increases losses and voltage issues
- MAOA improves classical AOA by enhancing stability and diversity
- MDAOA achieves the best overall performance through improved exploration
- Optimized placement strengthens voltage stability and system reliability

These findings confirm that the proposed framework, together with the optimization algorithms, provides an effective and practical approach for EVCS planning.

Conclusions and Future Research Directions

The rapid growth of electric vehicles has made charging infrastructure planning a critical challenge for modern power systems. Although EVCS deployment supports sustainable transportation, uncontrolled integration can introduce serious issues such as increased losses, voltage violations, transformer overloading, and reduced stability margins. Therefore, EVCS planning must be addressed as a joint optimization problem that considers both infrastructure needs and grid performance.

In this chapter, a multi-objective optimization framework was developed for EVCS placement in radial distribution networks. The problem formulation integrates three key criteria: active power loss, voltage deviation, and voltage stability index. This ensures that charging infrastructure decisions are not only efficient but also technically reliable.

To solve this problem, two improved variants of the Archimedes Optimization Algorithm were tested: MAOA and MDAOA. These methods were designed to overcome the limitations of classical AOA, particularly premature convergence and insufficient exploration.

Extensive validation using benchmark functions, the CEC 2017 suite, and engineering design problems confirmed that both MAOA and MDAOA improve algorithm performance. MAOA enhances convergence stability through adaptive control, while MDAOA achieves the best results by strengthening global exploration.

The effectiveness of the proposed methods was further demonstrated through case studies on IEEE-33, IEEE-69, and a real 10-bus distribution network. In all cases, optimized placement significantly reduced power losses, improved voltage profiles, and increased stability margins. These improvements are particularly important for distribution operators, as they reduce the need for costly network upgrades and enhance operational reliability.

A key takeaway is that EVCS placement cannot rely solely on demand-based decisions. Electrically unsuitable locations may lead to serious grid issues, even if they are attractive from a user perspective. Therefore, grid-aware optimization is essential. Among the tested methods, MDAOA showed the most consistent and robust performance, making it a strong candidate for practical applications.

Final Remarks

The results presented in this book demonstrate that advanced optimization techniques can effectively support EV charging infrastructure planning. The proposed MAOA and MDAOA algorithms show strong performance across both benchmark and real-world scenarios, with MDAOA providing the most reliable results.

As EV adoption continues to increase, distribution systems will face greater operational challenges. In this context, optimization-based and grid-aware planning approaches will play a crucial role in ensuring efficient, reliable, and sustainable electrification of transportation.

APPENDIX

Archimedes Optimization Algorithm

AOA is an optimization algorithm inspired by Archimedes' principle. An object is submerged in a liquid and pushed upwards by the buoyant force. This force is equal to the mass of the displaced liquid. According to this approach, every object submerged in a liquid tries to reach equilibrium. In this case, the buoyant force and the weight of the object are equal. This situation is presented in Equation 13. Equations 13-25 are taken from reference (84).

$$F_b = W_o, \qquad p_b v_b a_b = p_o v_o a_o \tag{13}$$

Here, F_b is the buoyant force, W_o , is the weight of the object, v is the volume, p is the density, b represents the liquid, o represents the submerged object, and a represents the acceleration or gravity.

In AOA, submerged objects form a population. The initial search is performed with random values, a common practice in most optimization algorithms. For each iteration, the density and volume values are updated until the algorithm's termination criteria are met. The four steps implemented in AOA can be listed as follows:

Step 1: Values of objects are randomly assigned as in Equation 14.

$$O_i = lb_i \times rand \times (ub_i - lb_i) \quad i = 1,2,\ldots,N \quad (14)$$

Here N is the population, O_i is the i-th object in N, lb_i is the lower bound and ub_i is the upper bound. Volume (vol) and density (den) values are initialized randomly as in Equation 15. The acceleration (acc_i) is initialized as in Equation 16 (84).

$$den_i = rand; \; vol_i = rand \quad (15)$$

$$acc_i = lb_i + rand \times (ub_i - lb_i) \quad (16)$$

Step 2: Density and volume are updated using Equation 17.

$$den_i^{t+1} = den_i^t + rand \times (den_{best} - den_i^t) \; ; \; vol_i^{t+1} = vol_i^t + rand \times (vol_{best} - vol_i^t) \; (17)$$

Here, den_{best} and vol_{best} best are the best volume and density values.

Step 3: The density factor is decreased while the transfer operator TF is increased. This enables the transition between the equilibrium state and phases (exploration-exploitation) after collisions. This is achieved with Equation 18.

$$TF = \exp\left(\frac{t - t_{max}}{t_{max}}\right) \quad (18)$$

Here, t represents the number of iterations. t_{max} is the maximum number of iterations. The density-reducing factor d, decreases over time using Equation 19.

$$d^{t+1} = \exp\left(\frac{t_{max} - t}{t_{max}}\right) - \left(\frac{t}{t_{max}}\right) \quad (19)$$

Step 4: Exploration phase: In this step, collisions occur according to the TF value. The object's acceleration (acc_i) is updated using Equation 20.

$$acc_i^{t+1} = \frac{den_{mr} + vol_{mr} \times acc_{mr}}{den_i^{t+1} \times vol_i^{t+1}} \tag{20}$$

den_i represents density and vol_i represents volume. acc_i, represents the acceleration of object i and mr represents random values.

Step 5: Exploitation phase: Depending on the TF value, no collision occurs. In this case, the acceleration of the object is updated using Equation 21.

$$acc_i^{t+1} = \frac{den_{best} + vol_{best} \times acc_{best}}{den_i^{t+1} \times vol_i^{t+1}} \tag{21}$$

Here, acc_{best} is the best acceleration value.

Step 6. Normalization of acceleration: In this step, the acceleration is very high when the solution is far from the global minimum, and it decreases over time in other cases. Therefore, $acc_{i,norm}^{t+1}$ adjusts the change in step size for each object. Equation 22 is used for this.

$$acc_{i-norm}^{t+1} = u \times \frac{acc_i^{t+1} - \min(acc)}{max(acc) - \min(acc)} + l \tag{22}$$

Here, u and l are the upper and lower values.

Step 7: Update step. In this step, positions are updated.

If TF is less than or equal to 0.5 (exploration phase), Equation 23 is used.

$$x_i^{t+1} = x_i^t + C_1 \times rand \times acc_{i-norm}^{t+1} \times d \times \left(x_{rand} - x_i^t\right) \tag{23}$$

Here, C_1 is equal to 2. If TF is greater than 0.5, the exploit phase is executed. Object positions are updated using Equation 24.

$$x_i^{t+1} = x_{best}^t \times F \times C_2 \times rand \times acc_{i-norm}^{t+1} \times d \times (T \times xbest - x_i^t) \quad (24)$$

Here C_2=6. $T = C_3 \times TF$. T increases over time in the range $[C_3 \times 0.3, 1]$. F represents the flag parameter used to change the direction of Equation 25.

$$F = \begin{cases} +1 \; if \; P < 0.5 \\ -1 \; if \; P > 0.5 \end{cases} \quad (25)$$

Step 8: Evaluation step. In this step, the fitness function is evaluated. If a better result is found, it is remembered.

Modified Archimedes Optimization Algorithms (MAOA and MDAOA)

The Archimedes Optimization Algorithm (AOA) offers an effective search mechanism but suffers from premature convergence and limited exploration in complex, high-dimensional problems. These limitations become more evident in EVCS placement, where the search space is highly nonlinear and includes many local optima shaped by network topology, load distribution, and voltage constraints.

In such problems, the algorithm must balance multiple objectives while preserving diversity long enough to explore alternative solutions. To address these issues, two improved variants are modified in the works of (85) and (86):

- Modified Archimedes Optimization Algorithm (MAOA)
- Dimension-Enhanced Modified Archimedes Optimization Algorithm (MDAOA)

Both methods aim to strengthen exploration, improve convergence behavior, and enhance robustness.

Modified Archimedes Optimization Algorithm (MAOA)

MAOA improves AOA by introducing a more flexible control over the exploration–exploitation balance. In classical AOA, this transition may occur too quickly, leading to early convergence. MAOA slows and adapts this transition, allowing broader exploration in early stages and gradual refinement later.

Two main improvements are introduced:

- Adaptive parameter control
- Perturbation-based diversification

Adaptive Parameter Control: Instead of fixed or linearly changing coefficients, MAOA updates parameters adaptively based on iteration progress. This allows the algorithm to maintain exploration longer when needed, particularly in complex multimodal landscapes.

For EVCS placement, this helps uncover non-obvious bus combinations that may lead to better overall performance.

Diversification via Perturbation: To prevent loss of diversity, MAOA applies controlled perturbations to selected solutions. These small variations allow the algorithm to escape local optima without disrupting promising solutions.

This is particularly useful in EVCS problems, where small changes in placement can significantly affect voltage profiles and losses.

MAOA Workflow

- Initialize population
- Evaluate fitness
- Update parameters and positions adaptively
- Apply perturbation to selected solutions

- Enforce constraints and update best solution
- Repeat until convergence

Dimension-Enhanced Modified AOA (MDAOA)

MDAOA extends MAOA by introducing a dimension-enhancement mechanism to improve search capability in high-dimensional problems.

In EVCS placement, the number of decision variables can be large, making the search space difficult to explore. MDAOA addresses this by increasing the effective search freedom of candidate solutions.

Dimension Expansion Mechanism: MDAOA temporarily expands the solution space by introducing auxiliary dimensions. These additional variables act as exploration aids, allowing solutions to move more freely across the search space. After exploration, solutions are projected back into the original variable space.

This approach improves diversity and enables the algorithm to explore distant regions more effectively.

Improved Acceleration Update: Unlike classical AOA, which relies heavily on the global best solution, MDAOA incorporates multiple reference solutions when updating acceleration. This reduces the dominance of a single solution and encourages more diverse search behavior.

As a result, the algorithm is less likely to converge prematurely.

Constraint Handling: MDAOA includes strict constraint handling to ensure feasibility. Violations such as out-of-range bus indices or excessive capacity are corrected, while infeasible solutions may be penalized. This ensures that only valid configurations are considered during optimization.

MDAOA Workflow

- Initialize population

- Evaluate fitness
- Update parameters and acceleration
- Expand dimensions for exploration
- Project solutions back to original space
- Apply constraint checks and update best solution
- Iterate until termination

Computational Considerations:The computational cost of MAOA and MDAOA mainly depends on population size and iteration count. In EVCS placement, load flow analysis dominates computation time.

The additional steps introduced (adaptive control, perturbation, and dimension expansion) are relatively lightweight. Therefore, both methods remain practical for real-world applications.

Discussion: The proposed modifications directly address key challenges in EVCS placement. The problem is highly sensitive, and small changes in station location can significantly affect voltage stability and losses.

MAOA improves performance by maintaining diversity and avoiding early convergence. MDAOA further enhances exploration by enabling broader search through dimension expansion.

Together, these methods provide more consistent and reliable solutions compared to classical AOA.

In summary:

- MAOA introduces adaptive parameter control and perturbation-based diversification
- MDAOA extends MAOA with dimension expansion and improved guidance mechanisms.

- Both methods reduce premature convergence and improve robustness.

The next section presents the validation of these algorithms using benchmark functions and practical case studies.

Benchmark Validation: Before applying an optimization method to real engineering problems, its performance must be verified using standard benchmark tests. These tests provide an objective way to evaluate search capability, convergence speed, stability, and robustness. In particular, they allow assessment under both unimodal (single optimum) and multimodal (multiple local optima) landscapes.

Authors in their work validated MAOA and MDAOA using three categories:

- Standard benchmark functions
- CEC 2017 benchmark suite
- Engineering design problems

This multi-level validation ensures that the methods are not only effective for EVCS placement but also reliable across different optimization scenarios.

Evaluation Criteria: Since metaheuristic algorithms are stochastic, performance is evaluated over multiple runs using statistical metrics:

- Best fitness value
- Mean fitness value
- Standard deviation
- Convergence behavior

Convergence curves are also analyzed to assess speed and stagnation. For engineering problems, feasibility is equally important, meaning solutions must satisfy all constraints.

Standard Benchmark Functions: The first validation stage uses classical benchmark functions such as Sphere, Rosenbrock, Rastrigin, Ackley, and Griewank. These functions represent different levels of complexity, dimensionality, and landscape characteristics.

Unimodal functions test exploitation capability, while multimodal ones evaluate exploration. Results show that MAOA improves the classical AOA by achieving lower average fitness values and reduced variability, indicating better stability.

MDAOA consistently outperforms both methods, demonstrating faster convergence and reduced stagnation. This confirms that the dimension-enhancement mechanism significantly improves global search performance.

CEC 2017 Benchmark Suite: To further evaluate performance, the CEC 2017 benchmark set is used. These functions are more complex, involving hybrid and composite structures that better represent real-world optimization landscapes.

Results indicate that classical AOA struggles due to premature convergence. MAOA provides noticeable improvements, particularly in reducing early stagnation. However, MDAOA achieves the best performance overall, producing the lowest average fitness values in most cases.

The results highlight that dimension enhancement allows better exploration of complex search spaces and improves robustness.

Engineering Design Problems: To assess real-world applicability, the algorithms are tested on five well-known engineering problems:

- Spring design
- Pressure vessel design

- Welded beam design
- Speed reducer design
- Three-bar truss design

These problems involve nonlinear constraints and coupled variables, making them more challenging than benchmark functions.

Across all cases, classical AOA produces feasible solutions but lacks consistency. MAOA improves stability, while MDAOA consistently delivers the best results in terms of both objective value and reliability.

In particular, MDAOA performs well in constrained problems, effectively avoiding infeasible regions and maintaining solution quality.

Statistical Validation and Robustness: Statistical tests confirm the superiority of the proposed methods. MDAOA achieves the best overall ranking and consistently lower standard deviation values, indicating stable and reliable performance.

This robustness is especially important for practical applications such as EVCS placement, where consistent results are more valuable than occasional high-quality solutions. Summary of Benchmark Validation: Overall, the benchmark results demonstrate that:

- Classical AOA performs adequately in simple problems but struggles in complex landscapes
- MAOA improves stability and reduces premature convergence
- MDAOA provides the best performance by enhancing exploration and maintaining diversity

These findings confirm that both modified AOA algorithms, particularly MDAOA, are well-suited for complex optimization tasks such as EVCS placement.

References

1. Ching Chuen Chan. The rise & Fall of electric vehicles in 1828-1930: Lessons learned. Proc IEEE. 2013;101(1):206–12.
2. TEIAŞ. Türkiye ve Kişi Başına Kurulu Güç - Brüt Üretim - Arz - Net Tüketiminin Yıllar İtibariyle Gelişimi [Internet]. 2018. Available from: https://www.teias.gov.tr/tr-TR/turkiye-elektrik-uretim-iletim-istatistikleri
3. Lopes JAP, Soares FJ, Almeida PMR. Integration of electric vehicles in the electric power system. Proc IEEE. 2011;99(1):168–83.
4. Shao S, Pipattanasomporn M, Rahman S. Challenges of PHEV penetration to the residential distribution network. 2009 IEEE Power Energy Soc Gen Meet PES ’09. 2009;1–8.
5. Denholm P, Short W. An Evaluation of Utility System Impacts and Benefits of Optimally Dispatched Plug-In Hybrid Electric Vehicles. NREL Rep noTP-620 [Internet]. 2006;(October):41. Available from: http://www.nrel.gov/docs/fy07osti/40293.pdf
6. Antalya Ticaret ve Sanayi Odası - Aylık göstergeler - Ocak 2015 [Internet]. Antalya; Available from: www.atso.org.tr
7. T.C. Kültür ve Turizm Bakanlığı Y ve İGM. 2019 Ocak Eylül Turizm İstatistikleri. 2019.
8. IEA. Global EV Outlook 2020: Technology Report. Glob EV Outlook 2020 Technol Rep. 2020;(June):39–85.
9. ODD. Pazar - Otomobil & Hafif Ticari, Genel Değerlendirme Aralık 2019 Erişim: 5 Ocak 2021 [Internet]. Available from: http://www.odd.org.tr/web_2837_1/neuralnetwork.aspx?type=35
10. ODD. Pazar - Otomobil & Hafif Ticari, Genel Değerlendirme Aralık 2020 Erişim: 5 Ocak 2021 [Internet]. Available from: http://www.odd.org.tr/web_2837_1/neuralnetwork.aspx?type=35
11. Moslehi K, Kumar R. A reliability perspective of the smart grid. IEEE Trans Smart Grid. 2010;1(1):57–64.
12. Ma G, Jiang L, Chen Y, Dai C, Ju R. Study on the impact of electric vehicle charging load on nodal voltage deviation.

Arch Electr Eng. 2017;66(3):495–505.
13. Singh M, Kar I, Kumar P. Influence of EV on grid power quality and optimizing the charging schedule to mitigate voltage imbalance and reduce power loss. Proc EPE-PEMC 2010 - 14th Int Power Electron Motion Control Conf. 2010;196–203.
14. Ucer E, Kisacikoglu MC, Cafer Gurbuz A. Learning EV Integration Impact on a Low Voltage Distribution Grid. In: IEEE Power and Energy Society General Meeting. IEEE; 2018. p. 1–5.
15. Nurmuhammed M, Karadağ T. Elektrikli Araç Şarj İstasyonlarının Konumlandırılması ve Enerji Şebekesi Üzerine Etkisi Konulu Derleme Çalışması. Gazi Univ J Sci PART A Eng Innov. 2021;8(2):30–45.
16. Phonrattanasak P, Leeprechanon N. Optimal Location of Fast Charging Station on Residential Distribution Grid. Int J Innov Manag Technol [Internet]. 2012;3(6):675–81. Available from: http://www.ijimt.org/show-40-537-1.html
17. Staats PT, Grady WM, Arapostathis A, Thallam RS. A statistical method for predicting the net harmonic currents generated by a concentration of electric vehicle battery chargers. IEEE Trans Power Deliv. 1997;12(3):1258–64.
18. Orr JA, Emanuel AE, Oberg KW. Current Harmonics Generated By a Cluster of Electric Vehicle Battery Chargers. SAE Prepr. 1981;584–9.
19. Lo EWC, Sustanto D, Fok CC. Harmonic load flow study for electric vehicle chargers. Proc Int Conf Power Electron Drive Syst. 1999;1(July):495–500.
20. Huang M, Huang S, Jiang J. Harmonic study of electric vehicle chargers. Beijing Jiaotong Daxue Xuebao/Journal Beijing Jiaotong Univ. 2008;32(5):85–8.
21. Balcells J, García J. Impact of plug-in electric vehicles on the supply grid. 2010 IEEE Veh Power Propuls Conf VPPC 2010. 2010;5–9.
22. Guo J, Zhao H, Shen Z, Wang A, Cao L, Hu E, et al. Research on Harmonic Characteristics and Harmonic Counteraction Problem of EV Charging Station. 2nd IEEE Conf Energy

Internet Energy Syst Integr EI2 2018 - Proc. 2018;
23. Bass R, Harley R, Lambert F, Rajasekaran V, Pierce J. Residential harmonic loads and EV charging. Proc IEEE Power Eng Soc Transm Distrib Conf. 2001;2(WINTER MEETING):803–8.
24. Harighi T, Bayindir R. Load Estimation Use in Electric Vehicle Charge Station Coordination in Different Node and Definite Area. 6th IEEE Int Conf Smart Grid, icSmartGrids 2018. 2019;264–71.
25. Khalkhali K, Abapour S, Moghaddas-Tafreshi SM, Abapour M. Application of data envelopment analysis theorem in plug-in hybrid electric vehicle charging station planning. IET Gener Transm Distrib. 2015;9(7):666–76.
26. Mwasilu F, Justo JJ, Kim EK, Do TD, Jung JW. Electric vehicles and smart grid interaction: A review on vehicle to grid and renewable energy sources integration. Renew Sustain Energy Rev. 2014;34:501–16.
27. Lund H, Kempton W. Integration of renewable energy into the transport and electricity sectors through V2G. Energy Policy. 2008;36(9):3578–87.
28. Sortomme E, El-Sharkawi MA. Optimal charging strategies for unidirectional vehicle-to-grid. IEEE Trans Smart Grid. 2011;2(1):131–8.
29. Kuzu B, Nurmuhammed M, Akdag O, Karadag T. A Simulation Study on Vehicle-to-Grid Implementation and Environmental Impacts. 6th Int Artif Intell Data Process Symp. 2022;
30. Tekdemir IG, Alboyaci B, Gunes D, Sengul M. A probabilistic approach for evaluation of electric vehicles' effects on distribution systems. 2017 4th Int Conf Electr Electron Eng ICEEE 2017. 2017;143–7.
31. Diaz C, Ruiz F, Patino D. Smart Charge of an Electric Vehicles Station: A Model Predictive Control Approach. 2018 IEEE Conf Control Technol Appl CCTA 2018. 2018;54–9.
32. Liu Z, Xie Y, Feng D, Zhou Y, Shi S, Fang C. Load forecasting model and day-ahead operation strategy for city-

located EV quick charge stations. IET Conf Publ. 2019;2019(CP764):1–6.
33. Güneş D, Tekdemir İG, Karaarslan MŞ, Alboyacı B. Elektrikli araç şarj istasyonu yüklerinin güvenilirlik indisleri üzerine etkilerinin incelenmesi. J Fac Eng Archit Gazi Univ. 2018;
34. Phonrattanasak P, Leeprechanon N. Optimal placement of EV fast charging stations considering the impact on electrical distribution and traffic condition. In: Proceedings of the 2014 International Conference and Utility Exhibition on Green Energy for Sustainable Development, ICUE 2014. Asian Institute of Technology; 2014. p. 19–21.
35. Galus MD, Vayá MG, Krause T, Andersson G. The role of electric vehicles in smart grids. Wiley Interdiscip Rev Energy Environ. 2013;2(4):384–400.
36. Nissan LEAF™ Charges up With SunPower. Erişim: 11 Ekim 2020 [Internet]. Available from: https://newsroom.sunpower.com/press-releases?item=122812
37. Tesla and SolarCity. (2016) Erişim: 10 Ekim 2020 [Internet]. Available from: https://www.tesla.com/blog/tesla-and-solarcity?redirect=no
38. Li CT, Ahn C, Peng H, Sun J. Integration of plug-in electric vehicle charging and wind energy scheduling on electricity grid. 2012 IEEE PES Innov Smart Grid Technol ISGT 2012. 2012;6–12.
39. Vaya MG, Andersson G. Integrating renewable energy forecast uncertainty in smart-charging approaches for plug-in electric vehicles. 2013 IEEE Grenoble Conf PowerTech, 2013. 2013;
40. Li CT, Ahn C, Peng H, Sun J. Synergistic control of plug-in vehicle charging and wind power scheduling. IEEE Trans Power Syst. 2013;28(2):1113–21.
41. Sehar F, Pipattanasomporn M, Rahman S. Demand management to mitigate impacts of plug-in electric vehicle fast charge in buildings with renewables. Energy [Internet]. 2017;120:642–51. Available from:

http://dx.doi.org/10.1016/j.energy.2016.11.118
42. Kempton W, Tomić J. Vehicle-to-grid power implementation: From stabilizing the grid to supporting large-scale renewable energy. J Power Sources. 2005;144(1):280–94.
43. Long YL, Li Y, Wang YH, Cao YJ, Jiang L, Zhou YC, et al. Impact of EV load uncertainty on optimal planning for electric vehicle charging station. Sci China Technol Sci. 2021;64(11):2469–76.
44. Etezadi-amoli M, Member S, Choma K, Stefani J, Member S. Rapid-Charge Electric-Vehicle Stations. IEEE Trans Power Deliv. 2010;25(3):1883–7.
45. Zeb MZ, Imran K, Khattak A, Janjua AK, Pal A, Nadeem M, et al. Optimal Placement of Electric Vehicle Charging Stations in the Active Distribution Network. IEEE Access. 2020;8:68124–34.
46. Deb S, Tammi K, Gao XZ, Kalita K, Mahanta P. A Hybrid Multi-Objective Chicken Swarm Optimization and Teaching Learning Based Algorithm for Charging Station Placement Problem. IEEE Access. 2020;8:92573–90.
47. Suganya S, Raja SC, Venkatesh P. Simultaneous coordination of distinct plug-in Hybrid Electric Vehicle charging stations: A modified Particle Swarm Optimization approach. Energy [Internet]. 2017;138:92–102. Available from: https://doi.org/10.1016/j.energy.2017.07.036
48. Hadian E, Akbari H, Farzinfar M, Saeed S. Optimal allocation of electric vehicle charging stations with adopted smart charging/discharging schedule. IEEE Access. 2020;8:196908–19.
49. Wu W, Lin Y, Liu R, Jin W. The multi-depot electric vehicle scheduling problem with power grid characteristics. Transp Res Part B Methodol [Internet]. 2022;155(October 2021):322–47. Available from: https://doi.org/10.1016/j.trb.2021.11.007
50. Pilz M, Al-Fagih L. Selfish energy sharing in prosumer communities: A demand-side management concept. 2019 IEEE Int Conf Commun Control Comput Technol Smart

Grids, SmartGridComm 2019. 2019;
51. Pilz M, Nebel JC, Ai-Fagih L. A Practical Approach to Energy Scheduling: A Game Worth Playing? Proc - 2018 IEEE PES Innov Smart Grid Technol Conf Eur ISGT-Europe 2018. 2018;
52. Ahmad F, Khalid M, Panigrahi BK. An enhanced approach to optimally place the solar powered electric vehicle charging station in distribution network. J Energy Storage [Internet]. 2021;42(July):103090. Available from: https://doi.org/10.1016/j.est.2021.103090
53. Sadhukhan A, Ahmad MS, Sivasubramani S. Optimal Allocation of EV Charging Stations in a Radial Distribution Network Using Probabilistic Load Modeling. IEEE Trans Intell Transp Syst. 2022;23(8):11376–85.
54. Le-ob-gbo O, Station C, Raval S, Natarajan T. A Novel Levy-Enhanced Opposition-Based Gradient-Based Optimizer (LE-OB-GBO) for Charging Station Placement. 2023;1–16.
55. Houssein EH, Deb S, Oliva D, Rezk H, Alhumade H, Said M. Performance of gradient-based optimizer on charging station placement problem. Mathematics. 2021;9(21):1–16.
56. Dharavat N, Sudabattula SK, Velamuri S, Mishra S, Sharma NK, Bajaj M, et al. Optimal Allocation of Renewable Distributed Generators and Electric Vehicles in a Distribution System Using the Political Optimization Algorithm. Energies. 2022;15(18).
57. Yuvaraj T, Devabalaji KR, Thanikanti SB, Pamshetti VB, Nwulu NI. Integration of Electric Vehicle Charging Stations and DSTATCOM in Practical Indian Distribution Systems Using Bald Eagle Search Algorithm. IEEE Access. 2023;11(May):55149–68.
58. Mohanty AK, Suresh Babu P, Salkuti SR. Optimal Allocation of Fast Charging Station for Integrated Electric-Transportation System Using Multi-Objective Approach. Sustain. 2022;14(22).
59. Bilal M, Rizwan M. Integration of electric vehicle charging stations and capacitors in distribution systems with vehicle-to-grid facility. Energy Sources, Part A Recover Util Environ

Eff [Internet]. 2021;00(00):1–30. Available from: https://doi.org/10.1080/15567036.2021.1923870
60. Golla NK, Sudabattula SK. Impact of Plug-in electric vehicles on grid integration with distributed energy resources: A comprehensive review on methodology of power interaction and scheduling. Mater Today Proc [Internet]. 2021;(xxxx). Available from: https://doi.org/10.1016/j.matpr.2021.03.306
61. Galiveeti HR, Goswami AK, Dev Choudhury NB. Impact of plug-in electric vehicles and distributed generation on reliability of distribution systems. Eng Sci Technol an Int J. 2018;21(1):50–9.
62. Green RC, Wang L, Alam M. The impact of plug-in hybrid electric vehicles on distribution networks: A review and outlook. Renew Sustain Energy Rev. 2011;15(1):544–53.
63. Bompard E, Ragazzi E, Tenconi A. The Greening of the Automotive Industry.
64. Clement-Nyns K, Haesen E, Driesen J. Analysis of the impact of plug-in hybrid electric vehicles on residential distribution grids by using quadratic and dynamic programming. World Electr Veh J. 2009;3(2):214–24.
65. Clement-Nyns K, Haesen E, Driesen J. The impact of vehicle-to-grid on the distribution grid. Electr Power Syst Res [Internet]. 2011;81(1):185–92. Available from: http://dx.doi.org/10.1016/j.epsr.2010.08.007
66. Clement-Nyns K. Impact of plug-in hybrid electric vehicles on Electricity systems. 2010.
67. Deb S, Tammi K, Kalita K, Mahanta P. Impact of electric vehicle charging station load on distribution network. Energies. 2018;11(1).
68. Ashique RH, Salam Z, Bin Abdul Aziz MJ, Bhatti AR. Integrated photovoltaic-grid dc fast charging system for electric vehicle: A review of the architecture and control. Renew Sustain Energy Rev. 2017;69(October 2016):1243–57.
69. SAE Electric Vehicle and Plug in Hybrid Electric Vehicle Conductive Charge Coupler. (2017) Erişim: 22 Temmuz 2018 [Internet]. Available from:

https://saemobilus.sae.org/content/J1772_201710/
70. IONITY orders 324 350kW EV chargers from ABB for second phase of expansion [Internet]. 2020. Available from: https://www.greencarcongress.com/2020/01/20200110-abb.html
71. Tesla. Supercharger [Internet]. 2023 [cited 2026 Feb 28]. Available from: https://www.tesla.com/supercharger
72. Kane M. Repsol Launches The Most Powerful Charging Station In Europe: 400 kW, Erişim [Internet]. Available from: https://insideevs.com/news/375020/repsol-most-powerful-charging-station-europe/
73. Chakravorty M, Das D. Voltage stability analysis of radial distribution networks. Int J Electr Power Energy Syst. 2001;23(2):129–35.
74. Li Y, Sun Y, Li K, Zhuang J, Liang Y, Pang Y. Analysis and suppression of voltage violation and fluctuation with distributed photovoltaic integration. Symmetry (Basel). 2021;13(10).
75. Liu J peng, Zhang T xi, Zhu J, Ma T nan. Allocation optimization of electric vehicle charging station (EVCS) considering with charging satisfaction and distributed renewables integration. Energy [Internet]. 2018;164:560–74. Available from: https://doi.org/10.1016/j.energy.2018.09.028
76. Hashim FA, Houssein EH, Hussain K, Mabrouk MS, Al-Atabany W. Honey Badger Algorithm: New metaheuristic algorithm for solving optimization problems. Math Comput Simul [Internet]. 2022;192:84–110. Available from: https://doi.org/10.1016/j.matcom.2021.08.013
77. Mirjalili S. SCA: A Sine Cosine Algorithm for solving optimization problems. Knowledge-Based Syst. 2016;96:120–33.
78. Talatahari S, Bayzidi H, Saraee M. Social Network Search for Global Optimization. IEEE Access. 2021;9:92815–63.
79. Holland JH. Genetic algorithms. SCIENTIFIC AMERICAN; 1992.
80. Kennedy J, Eberhart R. Particle Swarm Optimization. Ind Electron Handb - Five Vol Set. 2011;1942–8.

81. Arora S, Singh S. Butterfly optimization algorithm: a novel approach for global optimization. Soft Comput [Internet]. 2019;23(3):715–34. Available from: https://doi.org/10.1007/s00500-018-3102-4
82. Zhang M, Long D, Qin T, Yang J. A chaotic hybrid butterfly optimization algorithm with particle swarm optimization for high-dimensional optimization problems. Symmetry (Basel). 2020;12(11):1–27.
83. Kaur S, Awasthi LK, Sangal AL, Dhiman G. Tunicate Swarm Algorithm: A new bio-inspired based metaheuristic paradigm for global optimization. Eng Appl Artif Intell [Internet]. 2020;90(November 2019):103541. Available from: https://doi.org/10.1016/j.engappai.2020.103541
84. Hashim FA, Hussain K, Houssein EH, Mabrouk MS, Al-Atabany W. Archimedes optimization algorithm: a new metaheuristic algorithm for solving optimization problems. Appl Intell. 2021;51(3):1531–51.
85. Nurmuhammed M, Akdag O, Karadag T. A novel modified Archimedes optimization algorithm for optimal placement of electric vehicle charging stations in distribution networks. Alexandria Eng J. 2023;84:81–92.
86. Nurmuhammed M, Akdağ O, Karadağ T. Modified Archimedes optimization algorithm for global optimization problems: a comparative study. Vol. 1, Neural Computing and Applications. 2024.